ELSEVIER

NeuroImage

www.elsevier.com/locate/ynimg
NeuroImage 23 (2004) 213–223

White matter hemisphere asymmetries in healthy subjects and in schizophrenia: a diffusion tensor MRI study

Hae-Jeong Park,[a,b,c,d] Carl-Fredrik Westin,[b,c] Marek Kubicki,[a,c] Stephan E. Maier,[e] Margaret Niznikiewicz,[a] Aaron Baer,[a] Melissa Frumin,[a] Ron Kikinis,[c,e] Ferenc A. Jolesz,[c,e] Robert W. McCarley,[a] and Martha E. Shenton[a,c,*]

[a] *Clinical Neuroscience Division, Laboratory of Neuroscience, Boston VA Health Care System-Brockton Division, Department of Psychiatry, Harvard Medical School, Boston, MA 02301, USA*
[b] *Laboratory of Mathematics in Imaging, Department of Radiology, Brigham and Women's Hospital, Harvard Medical School, Boston, MA 02301, USA*
[c] *Surgical Planning Laboratory, Department of Radiology, Brigham and Women's Hospital, Harvard Medical School, Boston, MA 02301, USA*
[d] *Division of Nuclear Medicine, Department of Diagnostic Radiology, Yonsei University, College of Medicine, Seoul 120-752, South Korea*
[e] *MRI Division, Department of Radiology, Brigham and Women's Hospital, Harvard Medical School, Boston, MA 02301, USA*

Received 27 January 2004; revised 3 April 2004; accepted 28 April 2004
Available online 8 July 2004

Hemisphere asymmetry was explored in normal healthy subjects and in patients with schizophrenia using a novel voxel-based tensor analysis applied to fractional anisotropy (FA) of the diffusion tensor. Our voxel-based approach, which requires precise spatial normalization to remove the misalignment of fiber tracts, includes generating a symmetrical group average template of the diffusion tensor by applying nonlinear elastic warping of the demons algorithm. We then normalized all 32 diffusion tensor MRIs from healthy subjects and 23 from schizophrenic subjects to the symmetrical average template. For each brain, six channels of tensor component images and one T2-weighted image were used for registration to match tensor orientation and shape between images. A statistical evaluation of white matter asymmetry was then conducted on the normalized FA images and their flipped images. In controls, we found left-higher-than-right anisotropic asymmetry in the anterior part of the corpus callosum, cingulum bundle, the optic radiation, and the superior cerebellar peduncle, and right-higher-than-left anisotropic asymmetry in the anterior limb of the internal capsule and the anterior limb's prefrontal regions, in the uncinate fasciculus, and in the superior longitudinal fasciculus. In patients, the asymmetry was lower, although still present, in the cingulum bundle and the anterior corpus callosum, and not found in the anterior limb of the internal capsule, the uncinate fasciculus, and the superior cerebellar peduncle compared to healthy subjects. These findings of anisotropic asymmetry pattern differences between healthy controls and patients with schizophrenia are likely related to neuro-developmental abnormalities in schizophrenia.
Published by Elsevier Inc.

Keywords: Hemisphere asymmetry; Diffusion tensor MRI; Fractional anisotropy

Introduction

Hemisphere asymmetry in the brain has long been reported in healthy subjects in both neuroanatomy and function (Galaburda et al., 1978a; Geschwind, 1972; Geschwind and Galaburda, 1985a,b,c; Holinger et al., 2000; Kimura, 1973; Springer and Deutsch, 1998; Toga and Thompson, 2003). More particularly, neuroanatomical asymmetry, which has been presumed to be associated with functional lateralization (Amunts et al., 2000; Beaton, 1997; Kennedy et al., 1999; Moffat et al., 1998; Springer and Deutsch, 1998), has been found at the cytoarchitectronic level (Galaburda et al., 1978b; Rosen et al., 1993), in macrostructural volumes (Geschwind, 1972), and in morphometry (Sowell et al., 2002; Lancaster et al., 2003). Most typically, areas of macrostructural asymmetry include right frontal and left occipital petalias (Kennedy et al., 1999), the Sylvian fissures (Galaburda et al., 1978a; Sowell et al., 2002; Westbury et al., 1999), and the superior temporal plane, especially involving the planum temporale and Heschl gyrus (Anderson et al., 1999; Beaton, 1997; Galaburda et al., 1978b; Good et al., 2001; Moffat et al., 1998; Pujol et al., 2002; Watkins et al., 2001).

Neuroanatomical asymmetry in healthy subjects has been revealed not only in cortical gray matter, but also in white matter that interconnects cortical brain regions. White matter asymmetry has been explored primarily in studies of white matter volume of structures or in voxel-based concentration of white matter among subjects using structural MRI (Good et al., 2001; Pujol et al., 2002; Zhou et al., 2003). The recent advent of diffusion tensor magnetic imaging (DT-MRI) techniques (Basser et al., 1994), however, makes it possible to measure the quality of the neuronal fiber bundles within white matter regions of interest (ROI). For example, anisotropy of the diffusion tensor (Basser, 1995) provides information about the underlying structure of a given region, such as the myelination, density, and coherence of fibers. Accordingly, white matter

* Corresponding author. Department of Psychiatry-116A, VA Boston Healthcare System-Brockton Division, Harvard Medical School, 940 Belmont Street, Brockton, MA 02301. Fax: +1-508-586-0894.
E-mail address: martha_shenton@hms.harvard.edu (M.E. Shenton).
Available online on ScienceDirect (www.sciencedirect.com.)

1053-8119/$ - see front matter. Published by Elsevier Inc.
doi:10.1016/j.neuroimage.2004.04.036

asymmetry has been investigated using diffusion tensor images to explore anisotropic asymmetry in the uncinate fasciculi (Kubicki et al., 2002), the cingulate fasciculi (Kubicki et al., 2003), the anterior limb of internal capsule (Peled et al., 1998), and subinsular white matter (Cao et al., 2003). With the exception of the anterior limb of the internal capsule, the above regions of interest, that is, uncinate fasciculi, cingulate fasciculi, and subinsular white matter, all show a pattern of left-greater-than-right anisotropy in healthy controls.

Of note, an alteration that deviates from normal asymmetry has been explored in schizophrenia (Holinger et al., 2000) in neuroanatomy, including both postmortem studies of parahippocampal, fusiform gyri, and temporal lobe (Highley et al., 1998a,b, 1999; McDonald et al., 2000), and in MRI studies of temporal lobe, anterior cingulate gyrus, and frontal lobe (Takahashi et al., 2002; Turetsky et al., 1995), as well as in functions, including auditory processing such as mismatch negativity (Mohr et al., 2001; Rockstroh et al., 2001; Sommer et al., 2001; Youn et al., 2003). Alterations in white matter asymmetry in schizophrenia have also been exploited using DT-MRI, in studies looking at the cingulum bundle and uncinate fasciculus (Kubicki et al., 2002, 2003; Zhou et al., 2003). These latter studies follow closely in time the first DT-MRI studies of schizophrenia (Buchsbaum et al., 1998; Lim et al., 1999).

Methods used to explore white matter asymmetry, however, have been mostly based on measuring volume or anisotropy of a given region, that is, region of interest (ROI) in white matter structures. For example, early DT-MRI studies of white matter hemispheric asymmetry have included an evaluation of the internal capsule (Peled et al., 1998), the uncinate fasiculi (Kubicki et al., 2002), and the cingulate fasciculi (Kubicki et al., 2003) of healthy subjects and/or schizophrenia, and are based on an ROI method. Cao et al. (2003) also studied asymmetry of anisotropy of the subinsular white matter. The ROI-based approach requires a priori hypothesis to predefine the expected region of interest.

As an explorative method, the voxel-based strategy can be more helpful in identifying unanticipated or unpredicted/unhypothesized areas of neuroanatomical asymmetry. The voxel-based analysis of gray/white matter asymmetry has been conducted using voxel-based morphometry (VBM) (Good et al., 2001; Watkins et al., 2001) and deformation field analysis (Lancaster et al., 2003). The voxel-based analysis of white matter asymmetry has been conducted with structural MRI, where white matter throughout whole brain is regarded as homogeneous (Good et al., 2001). Such studies, using voxel-based morphometry to evaluate gray/white matter, have focused mainly on detecting the anatomical shape as well as regional volumetric difference. However, no study has been reported, as far as we know, on the asymmetry of white matter fiber bundles using voxel-based analysis of diffusion tensor images, where more sophisticated spatial normalization might be required to remove anatomical confounds, such as misalignment of narrow fiber bundles.

In this paper, we propose a new method for the voxel-based exploration of asymmetry of diffusion tensor using a higher order spatial normalization technique for tensor data (Guimond et al., 2002; Park et al., 2003a). This technique matches homologous locations in fiber bundles and minimizes potential misinterpretation of results that might otherwise be caused by misregistration. Using this method, we explore anisotropic asymmetry in diffusion tensor images of healthy subjects and patients with schizophrenia.

Methods

Subjects

Thirty-two normal male healthy subjects, with a mean age of 44 (30–55, SD: 6.2), were recruited from the general community. Twenty-three male patients with schizophrenia, with a mean age of 43 (28–53, SD: 7.2) were recruited from inpatient, day treatment, outpatient, and foster care programs at the VA Boston Healthcare System, Brockton, MA. The inclusion criteria for all subjects were right-handedness, no history of electroconvulsive shock treatment, no history of neurological illness or significant head trauma, no alcohol or drug dependence in the past 5 years, and no abuse within the past year, no medication with known effects on MR (such as steroids), verbal IQ above 75, English as a first language, and an ability and desire to cooperate with the procedures. In addition, healthy subjects were screened to exclude individuals who had a first-degree relative with an Axis I disorder, based on *DSM-IV* criteria. As part of a comprehensive neuropsychological battery, all subjects were evaluated using the verbal paired associate learning subtest of the Wechsler Memory Scale-3rd ed. (WMS) (Wechsler, 1997b), the Wisconsin Card Sorting Test (Nestor et al., 1998), the Trail Making Test, and the similarities subtest of the WAIS-III (Wechsler, 1997a). This research was approved by the local institutional review board of the VA Boston Healthcare System, and all subjects signed written informed consent before participation.

Acquisition of diffusion tensor images

Subjects were scanned using Line Scan Diffusion Imaging (LSDI) (Gudbjartsson et al., 1996; Maier et al., 1998; Mamata et al., 2002), which is comprised of a series of parallel columns lying in the image plane. The sequential collection of these line data in independent acquisitions makes the sequence largely insensitive to bulk motion artifact since no phase encoding is used and shot-to-shot phase variations are fully removed by calculating the magnitude of the signal.

A quadrature head coil was used on a 1.5 T GE Echospeed system (General Electric Medical Systems, Milwaukee, WI), which permits maximum gradient amplitudes of 40 mT/m. For each slice, six images with high diffusion-weighting (1000 s/mm^2) along six noncolinear and noncoplanar directions were collected. Two base line images with low diffusion-weighting (5 s/mm^2) were also collected and averaged. Scan parameters were as follows: rectangular FOV (field of view) 220 × 165 mm; 128 × 128 scan matrix (256 × 256 interpolated image matrix); slice thickness 4-mm; interslice distance 1-mm; receiver band width ±4 kHz; TE (echo time) 64 ms; effective TR (repetition time) 2592 ms; scan time 60 s per slice/section. A total of 31–35 coronal slices covering the entire brain were acquired, depending upon brain size.

Voxel-based analysis: asymmetry of diffusion tensor

The previous voxel-based analysis of hemisphere asymmetry has been performed by normalizing gray/white matter to a symmetric group average template and by comparing raw and flipped images of these normalized images (Good et al., 2001; Watkins et

al., 2001). Neuroanatomical correspondences between left and right hemisphere across subjects were determined by spatial normalization to a symmetric template.

The essential requirement for a voxel-based analysis of the diffusion tensor, including a study of white matter asymmetry, is to minimize the misinterpretation of statistical results due to misalignment. Most previous voxel-based DTI reports (Barnea-Goraly et al., 2003; Eriksson et al., 2001; Foong et al., 2002; Rugg-Gunn et al., 2001) have used a method similar to the one used for the voxel-based analysis of the structural scans called "voxel based morphometry".

In this study, we propose a method for voxel-based analysis of diffusion tensor image by reducing misalignment using a group template and higher order spatial normalization using multiple channel information.

Spatial normalization using multiple channel information of tensor field

Since diffusion tensor image contains underlying information (i.e., orientation, magnitude, and anisotropy of the tensor) of white matter, the registration needs to match these properties of the tensor to find correspondence between two images. We used a multiple channel demons algorithm (Guimond et al., 2001) to estimate deformation fields in the spatial normalization. This algorithm finds the displacement $v(x)$ for each voxel x of a target image T to match the corresponding location in a source image S. One channel of T2-weighted image and six channels of tensor components (Dxx, Dxy, Dxz, Dyy, Dyz, and Dzz) make it possible to match the shape, as well as the magnitude and orientation of local tensors between images. During the registration, the local tensor orientations were adjusted based on the deformation field as described by Alexander et al. (2001). Registration using the whole tensor information shows better registration performance than just using a channel of fractional anisotropy (FA) image or a channel of T2-weighted image (Park et al., 2003a).

Group atlas representing the mean of tensor field and mean of brain morphology

We created a group diffusion tensor atlas from 32 normal subjects by combining the average tensor field of all the normalized diffusion images and the average deformation field (Guimond et al., 2000; Park et al., 2003a). A diffusion image from healthy subjects was chosen as a temporary atlas, and all other images were registered to the temporary atlas with the adjustment of tensor orientation. The average of the registered diffusion images was resampled with the inverse of the average deformation field to achieve a morphological (shape) mean as well as an intensity (tensor) mean of the group. The average map was again used for the target atlas of the next iteration to reduce the effect of the first template chosen from a subject. Four iterations were used to create an average diffusion tensor map.

Symmetric atlas as a template for hemisphere correspondence

To create a symmetric template, both Good and Watkins groups (Good et al., 2001; Watkins et al., 2001) utilized the averaging of intensities from the original and flipped images of a scalar volume which may cause blurring of the template image due to hemispheric asymmetry. To address the issue of the blurring, we developed a novel method using a registration scheme with a multiple-channel demons algorithm (Guimond et al., 2000) to make a tensor image symmetric along the interhemispheric fissure, that is, midsagittal plane with reduced blurring effects. To make a diffusion tensor image I to be symmetric, the algorithm searches homologous locations between hemispheres by registering the tensor image I to its flipped image F, that is, $F(x_1, x_2, x_3) = I(-x_1, x_2, x_3)$, flipped along the midsagittal plane. As a result of the registration, the displacement $v(x)$ and the transformation $h(x)$, that is, $h(x)=x+v(x)$, at each voxel $x(x_1, x_2, x_3)$ of the image I can be found to match the corresponding anatomical location in its flipped image F. Using the transformation, $h(x)$, the registered image R was created by resampling the original diffusion tensor image I with the adjustment of the tensor orientation using the "Preservation of Principal Direction" algorithm described by Alexander et al. (2001). We averaged the flipped image, F, and the registered tensor image, R, which can be In this study, we propose a method for voxel-based analysis of diffusion tensor image by reducing misalignment using a group template and higher order spatial normalization using multiple channel information. Eq. (1).

$$R(x) = J_R(h(x)) \times I(h(x)) \tag{1}$$

$$\bar{S}(x) = 1/2[F(x) + R(x)]$$

where $J_R(h(x))\times$ indicates the adjustment of tensor orientation. Eq. (1) renders the average of tensor component images between corresponding positions of both hemispheres. The final step was to resample the average diffusion tensor image with the inverse of the mean displacement field as Eq. (2).

$$\bar{v}(x) = v(x)/2, \bar{h}(x) = x + \bar{v}(x) \tag{2}$$

$$S(x) = \bar{S}(\bar{h}^{-1}(x))$$

This step renders the corresponding tensors to be located at the symmetric positions along the midsagittal section of the brain and thus renders the average of anatomical shape between hemispheres.

Since the transformation from the left hemisphere to its corresponding right hemisphere and the transformation from the right hemisphere to its corresponding left hemisphere are not necessarily coincident, that is, $h(h(x)) \approx x$, at the final stage, we averaged both $S(x)$ and its flipped tensor image along the midsagittal section. Since $S(x)$ already is fairly close to symmetric, this final step did not introduce much blurring. This method combined both the average tensor field, that is, average magnitude and average direction of the tensor, and the average morphology, that is, shape, size, and position of the white matter, between left and right hemispheres.

Fig. 1 shows a coronal slice from a single diffusion tensor image (upper row) and a coronal slice from the symmetric average tensor template (lower row) derived from the 32 healthy subjects. The major eigenvector of each voxel is displayed with a line (in-plane component of the eigenvector) and color (from green to red, out-of-plane component of the eigenvector) on the background image of fractional anisotropy (FA), which is defined below:

$$\mathrm{FA} = \frac{\sqrt{(l_1 - l_2)^2 + (l_2 - l_3)^2 + (l_1 - l_3)^2}}{\sqrt{2}\sqrt{l_1^2 + l_2^2 + l_3^2}} \tag{3}$$

where l_1, l_2, l_3 are eigenvalues of the tensor from larger to lower values, respectively.

Spatial smoothing of fractional anisotropy

To reduce the effect of misregistration in spatial normalization and to increase signal to noise ratio, smoothing with Gaussian filter is usually used before applying statistics. We considered two

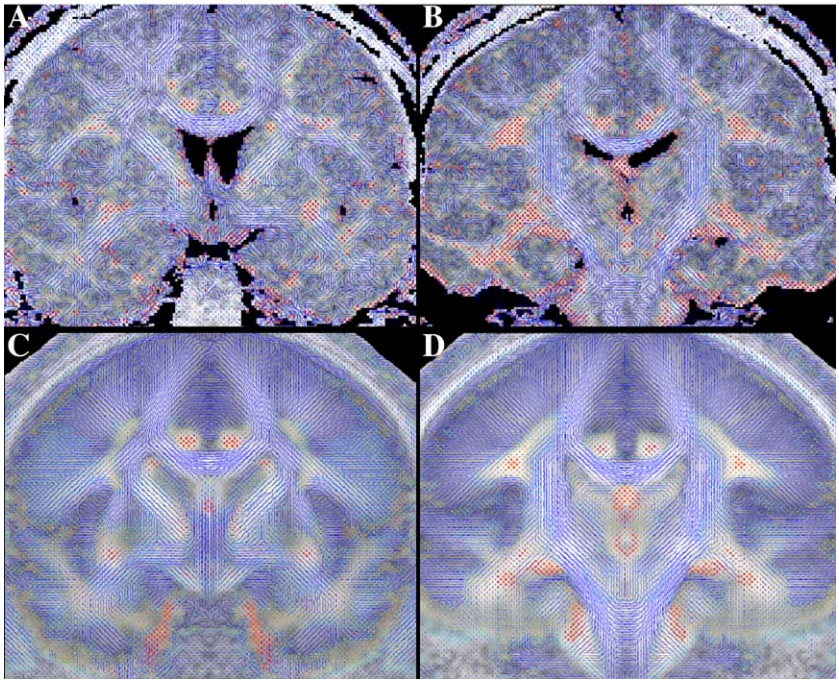

Fig. 1. Coronal slices from a single diffusion tensor image (upper panel, A and B) and coronal slices from the symmetric average tensor template derived from 32 healthy subjects (lower panel, C and D). Major eigenvectors for each voxel are displayed with line (in-plane component of the eigenvector) and color (from green to red, out-of-plane component of the eigenvector) on the background image of fractional anisotropy.

approaches to smooth the fractional anisotropy: (1) the fractional anisotropy from the Gaussian filtered tensor field and (2) the Gaussian filtered fractional anisotropy derived from the raw tensor field. The former, which is a local averaging of the tensor field with a Gaussian mask, is a powerful way to measure the local coherence of the fibers and results in stable estimates of the tensor directionality in the area where there is a clear bias in one direction (Westin et al., 2002). However, it may not be optimal for reducing the effect of misalignment for statistical analysis of fractional anisotropy. For example, the application of Gaussian filter on tensor fields where neighboring fiber bundles are perpendicular to each other, such as in the cingulum bundle and corpus callosum, will result in mixing tensors of different orientation and thus reduced fractional anisotropy in that region. The two smoothing operations are thus very different. The first case, smoothing the tensor data, should be viewed as a data relaxation operation, where tensor data information is spread spatially. The second case of smoothing FA should be viewed as a feature relaxation operation, where the derived feature here is FA, and the smoothing spreads this information spatially. It is not surprising that the results are different since the calculation of FA is a nonlinear operation. However, sometimes the two operations give similar results. In regions of coherent tensors, anisotropic or not, the two methods tend to perform similarly, but in regions of mixed tensors, they give very different results. Smoothing tensor data reduce the FA in such regions. This is especially noticeable along the boundary of white matter and in regions of fiber crossings or differently oriented fiber bundles at close proximity. However, smoothing the fractional anisotropy spreads the information spatially and thus reduces the effect of registration errors in the statistical evaluation of fiber bundle anisotropy. Therefore, we have chosen to use the latter method, that is, smoothing the fractional anisotropy of normalized tensor images, which was registered to a symmetric template.

The kernel size of Gaussian smoothing can be determined by weighting the need for reduction of anatomical misalignment and increase of the signal to noise ratio versus the loss of spatial resolution. Previous studies have used different size of Gaussian kernels, for example, full width at half maximums (FWHM) of 4 × 4 × 4 mm (Barnea-Goraly et al., 2003), 8 × 8 × 8 mm (Eriksson et al., 2001), and 12 × 12 × 12 mm (Burns et al., 2003). Fig. 2 shows example of the two filtering approaches defined above with different kernel sizes of FWHMs 3 × 3 × 3 mm, 6 × 6 × 6 mm, and 9 × 9 × 9 mm. In this study, we applied Gaussian smoothing with FWHM of 6 × 6 × 6 mm to all normalized fractional images. Note how the FA from the smoothed tensor field is darker in the interfaces between bundles having different fiber directions.

Statistical analysis of diffusion anisotropy between hemispheres

The statistical analysis of hemispheric asymmetry can be summarized as follows:

(1) We normalized all tensor images to a symmetric DT-MRI template.
(2) We smoothed the fractional anisotropy images with a Gaussian filter of FWHM 6 × 6 × 6 mm.
(3) We created left/right flipped smoothed FA images along the interhemispheric fissure, that is, midline of the symmetric atlas.
(4) We calculated statistics and created a statistic map of anisotropic difference at each voxel between the original FA images and their flipped images.
(5) We defined the threshold and the cluster extent of the statistic maps. To evaluate the effect of smoothing kernel size on statistical results, we also applied the same statistical procedures to the Gaussian filtered images with both FWHM 3 × 3 × 3 mm and 9 × 9 × 9 mm.

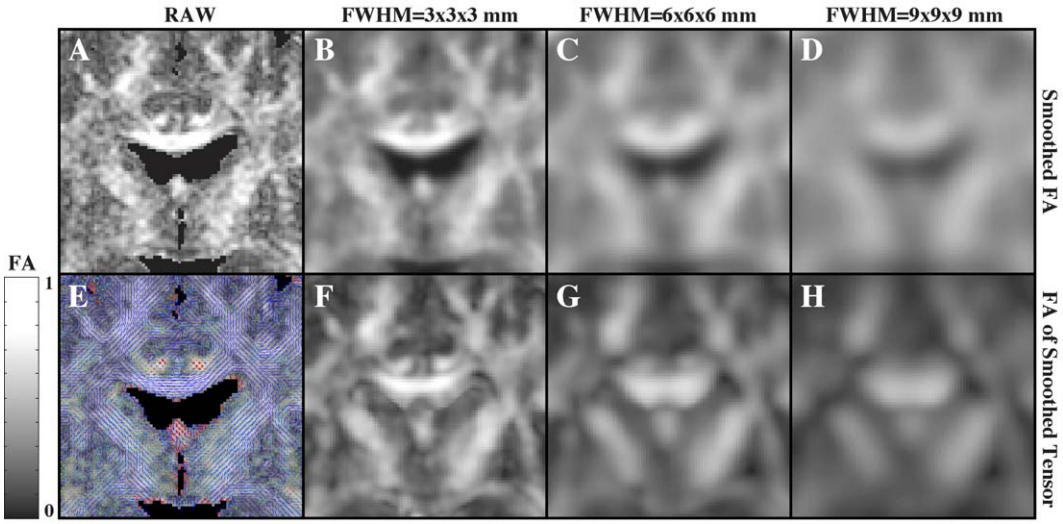

Fig. 2. Smoothing methods and kernel size for fractional anisotropy. The original raw fractional anisotropy map and its 2D glyphs display are shown in panels A and D. Coronal slices of Gaussian filtered fractional anisotropy (B, C, and D) and coronal slices of fractional anisotropy of Gaussian filtered tensor field (F, G, and H) have been displayed with full-width half-maximum FWHMs of 3 × 3 × 3 mm, 6 × 6 × 6 mm, and 9 × 9 × 9 mm.

We conducted statistical analysis for each voxel within the white matter of the average image of normalized images using a pairwise *t* test, since the sample sizes were sufficiently large (32 for NC and 23 for SZ) and since a test of normality, using the Lin-Mudholkar normality test (Lin and Mudholkar, 1980) at each voxel, showed no significant evidence for non-Gaussian distribution of fractional anisotropy in the white matter. At a threshold $P < 0.005$ without a correction for multiple comparisons, clusters

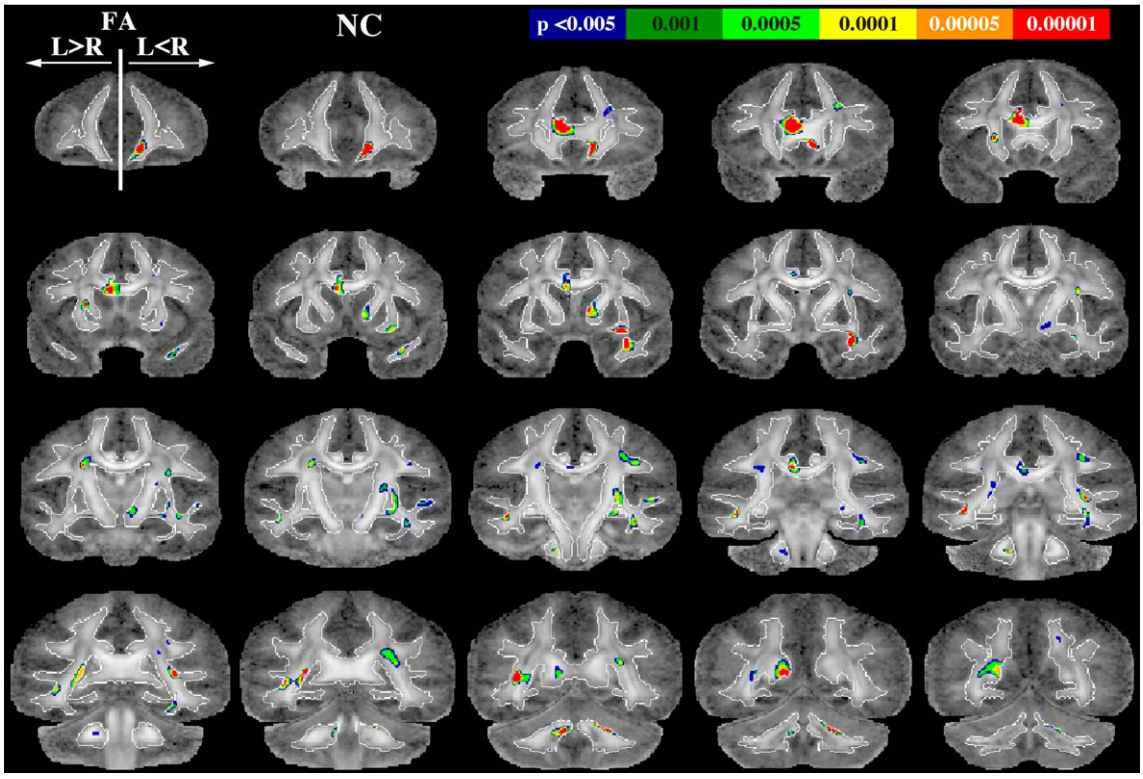

Fig. 3. The statistical map of the statistically significant asymmetric regions in fractional anisotropy of healthy subjects. Colored dots in the left hemisphere (neurological convention) indicate voxels with higher fractional anisotropy in the left hemisphere than right, and colored dots in the right hemisphere indicate voxels with higher fractional anisotropy in the right hemisphere than the left. The white thin lines in the images show boundary voxels where a pairwise *t* test was conducted.

consisting a minimum of 60 contiguous voxels were considered to show asymmetry statistically.

Results

Fig. 3 shows the statistical map of the significantly asymmetric regions in fractional anisotropy of healthy subjects thresholded by $P < 0.005$, $P < 0.001$, $P < 0.0005$, $P < 0.00005$, and $P < 0.00001$ with a cluster size of >60 voxels at $P < 0.005$. Colored dots in the left hemisphere (neurological convention, left hemisphere on the left side of the picture) indicate voxels with higher fractional anisotropy in the left hemisphere than right, and colored dots in the right hemisphere indicate voxels with higher fractional anisotropy in the right hemisphere than the left. The white thin lines in the images, which were extracted from the template, show boundary voxels where a pairwise t test was conducted.

Table 1 summarizes hemispheric asymmetry from fractional anisotropy in healthy subjects. Left-greater-than-right asymmetry was found in genu, rostrum, and splenium of the corpus callosum, cingulum bundle, optic radiation, and superior cerebellar peduncles, while right-greater-than-left asymmetry was found at the prefrontal regions of anterior limb of the internal capsule fibers, the uncinate fasciculus, internal capsule, and the superior and inferior aspect of the arcuate fasciculus (superior longitudinal fasciculus and inferior longitudinal fasciculus).

Right-greater-than-left asymmetry of the uncinate fasciculus appears in the stem and the inferior aspect of the fiber bundle.

Table 1
Hemispherical asymmetry of fractional anisotropy in healthy subjects

Description of extent of cluster		Talairach coordinates of most significant voxel (x, y, z)	Cluster size[a]	z-Score
Cingulum bundle and CC	L > R	−7.8, 35.5, 10.4	946	5.81
Optic radiation	L > R	−36.0, −44.1, 8.0	614	5.81
Superior cerebellar peduncle	L > R	−7.8, −51.8, −32.9	161	5.00
Splenium (CC)	L > R	−11.4, −49.9, 11.2	173	4.60
Posterior limb IC × SLF	L > R	−23.7, −5.3, 24.1	140	4.36
Medial prefrontal white matter	L > R	−21.9, 23.8, 1.0	78	4.70
Anterior prefrontal white matter	L < R	2.7, 27.7, −4.1	406	6.14
Uncinate fasciculus	L < R	25.6, −1.4, −17.9	305	5.80
Splenium (CC) × posterior SLF	L < R	32.6, −30.5, 3.4	262	5.29
Inferior longitudinal fasciculus	L < R	32.6, −22.7, −15.5	206	4.54
SLF	L < R	32.6, −16.9, 27.0	200	3.97
Anterior limb IC	L < R	6.2, 6.4, 3.6	129	4.65
Posterior limb IC	L < R	6.2, −11.1, −9.6	80	3.72
Arcuate fasciculus and SLF complex	L < R	27.4, −1.4, 17.3	69	4.05
Superior prefrontal white matter	L < R	18.6, 31.6, 26.0	62	3.77

CC, corpus callosum; SLF, superior longitudinal fasciculus; IC, internal capsule; ×, crossing area of fiber bundles.
[a] Cluster size is in the unit of voxel.

However, we did not find significant left-greater-than-right asymmetry at the uncinate fasciculus. Having in mind the previous report (Kubicki et al., 2002), we explored the effect of smoothing kernel size on the results. Fig. 4 demonstrates three consecutive coronal slices of the statistical asymmetry maps in healthy subjects derived from three different Gaussian kernel sizes, that is, FWHM of 3 × 3 × 3 mm, 6 × 6 × 6 mm, and 9 × 9 × 9 mm. For this particular structure, statistical maps with smaller smoothing filter with FWHM 3 × 3 × 3 mm (Fig. 4C) demonstrate the left-greater-than-right asymmetry in controls in superior portion of uncinate fasciculus, which is consistent with the previous manual result (Kubicki et al., 2002) measured at the similar location. Since the uncinate fasciculus is coherent only for a very short distance, the smoothing kernel of 6 × 6 × 6 mm FWHM might enhance the partial volume effect by including low anisotropy voxels located outside the stem of this fiber bundle, reducing the statistical power in this region. In the map of larger smoothing kernel size with FWHM 9 × 9 × 9 mm, the anisotropy of the cingulum bundle was smeared into neighboring low anisotropy structures, and the asymmetry was not detected significantly in the cingulum bundle (Figs. 4G–I).

Note that significant asymmetry was detected at fiber crossing areas, such as left-higher-than-right in the medial regions where the superior longitudinal fasciculus and fibers from posterior limb of the internal capsule are crossing, and right-higher-than-left in the posterior regions where corpus callosum fibers (splenium) cross the superior longitudinal fasciculus.

The statistical asymmetry map of fractional anisotropy in schizophrenics is shown in Fig. 5 and is summarized at Table 2. Here, it is clear that patients with schizophrenia show reduced hemispheric asymmetry in fractional anisotropy compared with healthy subjects.

We found anisotropy asymmetry in patients with schizophrenia at cingulum bundle, callosal fibers, optic radiation, and middle and posterior portions of superior longitudinal fibers. Normal asymmetry in controls was not found at anterior limb of the internal capsule and at the uncinate fasciculus.

Fig. 6 shows the results of our study superimposed on the three-dimensional model of white matter fiber tracts, obtained with the method described elsewhere (Park et al., 2003b). The colors in the fiber bundles are derived from the voxel's z-values and show left–right asymmetry. The portion of the figure above the yellow line illustrates left-greater-than-right FA asymmetry similar to Figs. 3 and 5, whereas the portion of the figure below the line shows FA asymmetry in the opposite direction (i.e., right-greater-than-left). These z-values for the cingulum bundle and the anterior portion of the CC clearly demonstrate a left-greater-than-right asymmetry in controls that is present, albeit, reduced in schizophrenia.

Discussion

Voxel-based analysis of asymmetry of diffusion tensor in white matter

For voxel-based analysis, the basic requirement is to correctly find anatomical correspondence between images. In the analysis of gray matter, each gyrus and sulcus can be mapped to the corresponding template structure based only on the signal intensity obtained from T1- or T2-weighted images. However, structural

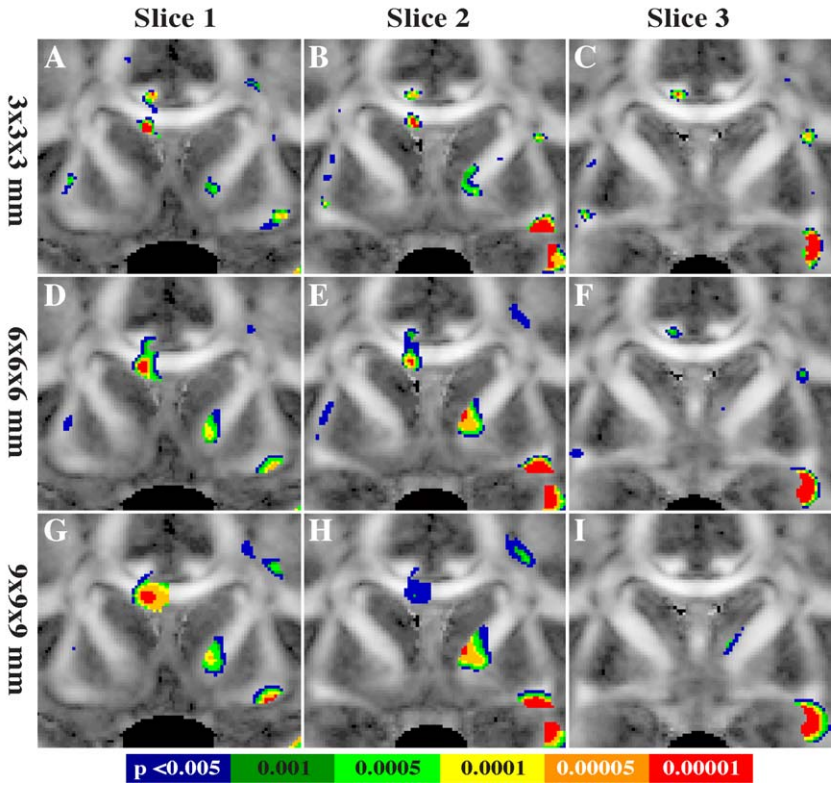

Fig. 4. Statistical asymmetry map of fractional anisotropy in healthy subjects: similarity and difference between Gaussian kernel size of 3 × 3 × 3 mm, 6 × 6 × 6 mm, and 9 × 9 × 9 mm in FWHM. All voxels having lower *P* values than 0.005 were displayed without application of exclusion criteria of the cluster size.

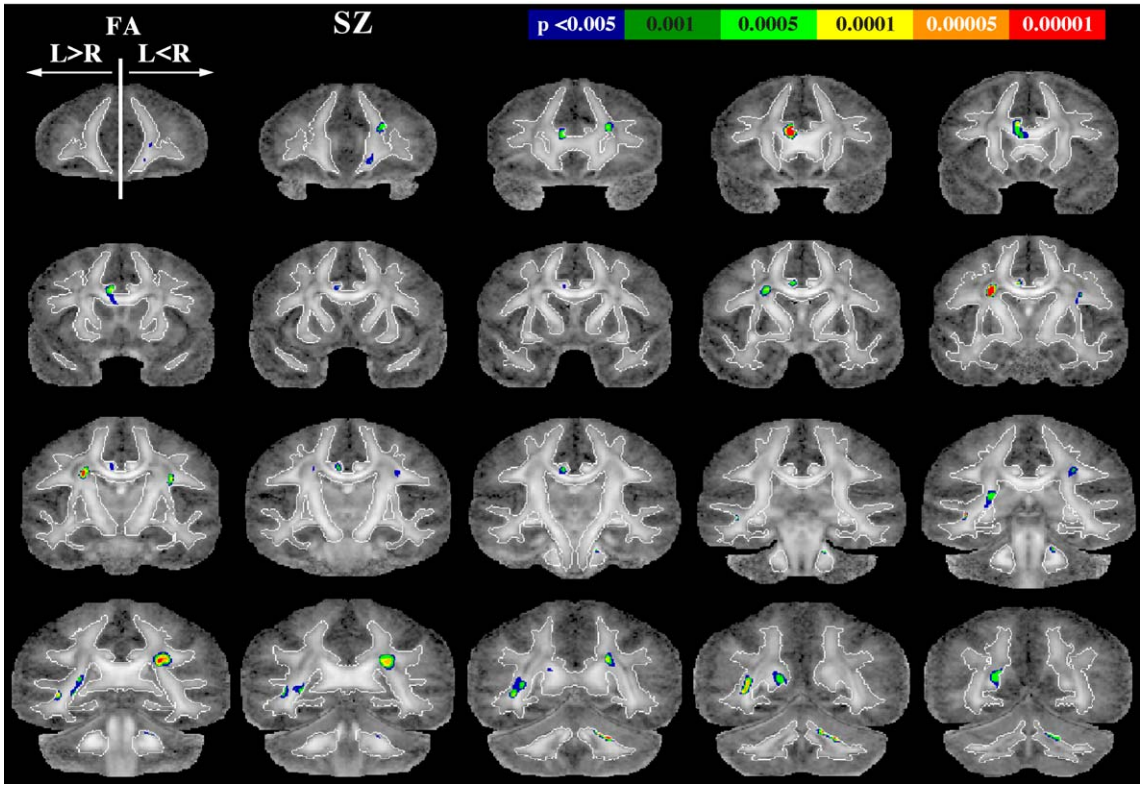

Fig. 5. The statistical map of the statistically significantly asymmetric regions in fractional anisotropy in schizophrenics. Colored dots in the left hemisphere (neurological convention) indicate voxels with higher fractional anisotropy in the left hemisphere than right, and colored dots in the right hemisphere indicate voxels with higher fractional anisotropy in the right hemisphere than the left.

Table 2
Hemispherical asymmetry of fractional anisotropy in schizophrenic subjects

Description of extent of cluster		Talairach coordinates of most significant voxel (x, y, z)	Cluster size[a]	z-Score
Cingulum bundle and CC	L > R	−7.8, 29.7, 13.6	426	6.05
Optic radiation	L > R	−37.8, −30.5, −1.8	455	4.49
Posterior limb IC × SLF	L > R	−23.7, 0.6, 24.4	177	5.15
Splenium (CC)	L > R	−18.4, −53.8, 16.3	175	3.61
Splenium (CC) × posterior SLF	L < R	20.3, −32.4, 24.5	348	4.46
Anterior prefrontal white matter	L < R	13.3, 49.1, −3.0	93	3.50
Superior prefrontal white matter	L < R	18.6, 35.5, 17.4	83	3.76
Arcuate fasciculus and SLF complex	L < R	27.4, −5.3, 22.3	78	3.83

CC, corpus callosum; SLF, superior longitudinal fasciculus; IC, internal capsule; ×, crossing area of fiber bundles.
[a] Cluster size is in the unit of voxel.

MR images, which have been generally used for previous voxel-based studies of fractional anisotropy (Barnea-Goraly et al., 2003; Burns et al., 2003; Eriksson et al., 2001; Foong et al., 2002; Rugg-Gunn et al., 2001), do not include information essential for finding anatomical correspondence of the white matter structures (namely, fiber tract's orientation and organization) and thus might not be appropriate for finding precise anatomical correspondence in DT-MRI. This is why we used a more complex registration approach that utilizes multiple channel tensor information to match anatomical correspondence between subjects and between hemispheres instead of using fractional anisotropy or T2-weighted images, even for the analysis of fractional anisotropy.

In addition, as a result of the better coregistration of the corresponding anatomical structures between subjects and between hemispheres, and as a result of the combination of the averaged deformation field, our mean image (symmetric template further used for normalization) was both less blurred and more representative of the morphology of the group than is the case for more traditional voxel-based studies. In spite of our strategy for better registration, by looking at the overlap of normalized white matter segmentations thresholded with FA > 0.3, we found some registration errors in the boundary of narrow fiber bundles. These errors were most likely due to anisocubic voxels (0.8594 × 5 × 0.8594 mm, an interpolated image voxel unit of the original scan unit 1.7 × 5 × 1.7 mm), relatively low resolution tensor images that we used for the analysis, as well as due to presumable interindividual variations of topology.

To reduce the effect of normalization errors on the statistical analysis, Gaussian smoothing was applied to the normalized fractional anisotropy images. As was demonstrated in Fig. 4, a smaller smoothing kernel can be used to detect asymmetry even in narrow fiber bundles or in the fibers in close proximity to neighboring fibers, although using such a smaller smoothing kernel increases the probability of a type I error. On the other hand, a larger smoothing kernel increases robustness to errors resulting from either registration or artifacts, or both, as it sacrifices spatial resolution. Thus, the smoothing kernel size should be small enough to detect narrow structures but large enough to be robust to errors. Finally, although we determined smoothing kernel size by experiment in our case, a more generalized method using an appropriate model needs to be further researched.

Since diffusion tensors characterize diffusion strength and orientation much better than the FA indices, tensor asymmetry comparison, instead of FA asymmetry comparison, would be the appealing and logical choice. From a clinical perspective, however, asymmetry in the tensor of one voxel or of neighboring voxels is not easy to interpret. On the other hand, FA has a relatively clearer meaning; that is, it reflects the fiber bundle quantity underlying the voxel, such as myelination, coherence, and/or density.

Asymmetry of fractional anisotropy in white matter of normal controls and patients diagnosed with schizophrenia

We found anisotropic asymmetry differences for the cingulum bundle, which showed left-higher-than-right anisotropy in healthy subjects. This finding is consistent with a previous finding from our group based on an ROI method (Kubicki et al., 2003). We also noted an anisotropic asymmetry in healthy controls in the anterior limb of the internal capsule and extended fibers that connect orbital frontal regions, which showed higher anisotropy in the right than left and which is also consistent with a previous finding in the literature (Peled et al., 1998).

The subinsular regions, reported to be left-greater-than-right asymmetry (Cao et al., 2003) using manual ROI methods, did not

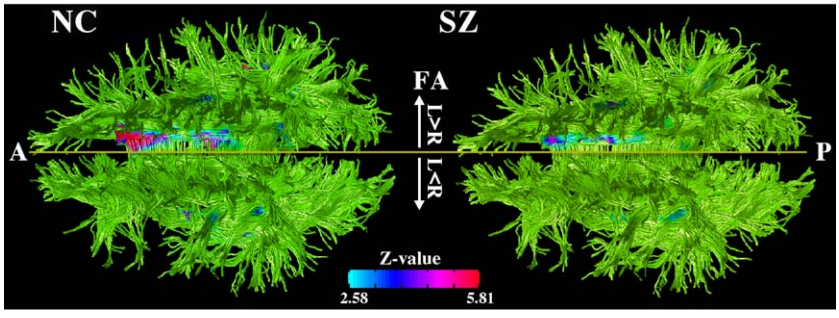

Fig. 6. Asymmetry of fractional anisotropy (FA) in normal controls (NC) and patients with schizophrenia (SZ) superimposed on the three-dimensional tractography. The colors in the fiber bundles are derived from the left−right asymmetry z-values displayed in Figs. 3 and 5. The portion of the figure above the yellow line illustrates left-greater-than-right FA asymmetry, while the portion below shows FA asymmetry in opposite direction (right-greater-than-left). A indicates anterior; P, posterior.

show a significant asymmetry ($P < 0.001$) but did show a tendency toward asymmetry ($P < 0.005$), as depicted in Fig. 4. This slight discrepancy might be due to the narrow structure of the subinsular region and thus due to low spatial alignment after normalization of this region.

In our results, in healthy controls, uncinate fasciculus was compromised of fibers showing two different patterns of asymmetry (right-greater-than-left in the middle and inferior portion, and left-greater-than-right in the superior portion at the smoothed FA images with FWHM 3 × 3 × 3 mm). Previous DT-MRI report of Kubicki et al. (2002), which investigated uncinate fasciculus by measuring fractional anisotropy at a center point of each tract at most perpendicular to the coronal plane, was able to demonstrate only the second pattern of asymmetry, that is, left-greater-than-right fractional anisotropy in control subjects, and no asymmetries in schizophrenia. In postmortem study of Highley et al. (2002), both schizophrenia and controls showed right-greater-than-left asymmetry of cross-sectional area and fiber number in the uncinate fascicle. Therefore, the asymmetry of the uncinate fasciculus is still controversial, and further study is necessary for both control group and schizophrenia group.

In schizophrenia, the overall pattern of asymmetry findings was similar to that of healthy controls but showed reduced asymmetry. More specifically, in the uncinate fasciculus and in the anterior limb of the internal capsule, the asymmetry pattern observed in controls was not found in schizophrenia subjects, while reduced asymmetry was observed in the anterior part of the corpus callosum in schizophrenics compared to control subjects. Anisotropic asymmetry was also observed in the cingulum bundles of schizophrenia, which corresponds to a previous report by our group (Kubicki et al., 2003).

The cingulum bundle is the most prominent connection between limbic structures and is known to consolidate information by interconnecting thalamus, prefrontal, parietal, temporal lobes (including amygdala, hippocampus, and parahippocampal gyrus) with cingulate gyrus. The anisotropic asymmetry of the cingulum bundle indicates the lateralization of brain function, which appears to be similar in both normal controls and schizophrenics, that is, left greater than right.

The anterior limb of the internal capsule connecting prefrontal association cortex and subcortical nuclei comprise frontal-subcortical feedback loops. The asymmetry of right>left in healthy subject is not found in schizophrenia. Absence of anisotropic asymmetry in schizophrenia might be related to functional disconnection as well as a disturbance in thalamic filtering in this group. Zhou et al. (2003) reported right-greater-than-left asymmetry in the volumes of anterior limb in both controls and patients with schizophrenia, although the schizophrenia group showed significantly increased asymmetry compared with controls. However, our voxel-based approach showed reduced, right-greater-than-left asymmetry of fractional anisotropy in schizophrenia.

Of further note, the uncinate fasciculus, the major fiber tract connecting the inferior frontal and anterior temporal lobes (Ebeling and von Cramon, 1992), is known to play a role in decision making as well as in the retrieval of semantic and episodic memory. The absence of asymmetry of fractional anisotropy in the uncinate fasciculus in schizophrenia thus suggests an abnormality in the integrity of the fibers connecting the inferior frontal and anterior temporal regions (Akbarian et al., 1996; Deakin and Simpson, 1997).

In our study, one of the most significant asymmetry regions for controls was observed for the anterior portion of the corpus callosum. This asymmetry was also found but in a reduced way in patients with schizophrenia. Of interest here, we note that the anterior corpus callosum interconnects the prefrontal lobes of both hemispheres (Makris et al., 1999) and is reported to be involved in the higher order transfer of semantic information (Gazzaniga, 2000). Furthermore, thin fibers that are lightly myelinated, of which a large majority are believed to interconnect association cortex, are most dense in the anterior corpus callosum (genu), relative to total corpus callosum (Aboitiz et al., 1992). Moreover, heterotopic connections between nonequivalent cortical regions in each hemisphere are known to be numerous and widespread (Di Virgilio and Clarke, 1997; Toga and Thompson, 2001). Thus, these neuroanatomical and functional differences in the anterior part of the corpus callosum may play a critical role in our finding of fractional anisotropic asymmetry of the anterior corpus callosum.

Note that we did not directly compare asymmetry difference between healthy subjects and schizophrenic subjects in this study. While we considered using an asymmetric index, as for example, (L − R) / (L + R) / 2, such asymmetry indices assume that the normalization error is not significantly different between groups when matching homologous points. For the schizophrenic group, this assumption may not be true. In fact, when we checked the within-group overlap of normalized white matter segmentations, derived from individual subjects of each group using a threshold of 0.3 for FA, the overlap of schizophrenics was less than that of healthy subjects especially in the narrow fiber structures. This might be associated with the high interindividual anatomical variability known to exist in schizophrenia, a very heterogeneous group. For this reason, we decided to use a within-group comparison of hemisphere asymmetry.

Interpretation of fractional anisotropy asymmetry between hemispheres

Although we found hemispheric asymmetry of fractional anisotropy in healthy subjects and, to a much lesser extent, in schizophrenia, the interpretation of these results requires some caution. For example, since fractional anisotropy represents a combination of fiber size, density, myelination, and fiber coherence, any of these factors can influence the results. Moreover, fractional anisotropy can be influenced by fiber crossings, especially in areas where two or more major bundles cross. One such area lies lateral to the genu of the corpus callosum, where fibers coming out of the corpus cross with internal capsule radiation fibers and fibers of the superior longitudinal fasciculus. Therefore, fractional anisotropy differences do not necessarily indicate differences in indices of the anatomical connectivity, such as the number of fibers or myelination. Likewise, the lack of FA differences does not necessarily indicate unambiguous connectivity. The interpretation should be further researched.

One potential approach to increase the specificity of DT-MRI asymmetry studies is to use fiber tractography. We have applied such an approach to explore asymmetry of neural connectivity in both controls and schizophrenia by measuring mean fractional anisotropy along the fibers (Park et al., 2003b). However, exploration of asymmetry using fiber tractography can only be used in an exploratory manner since there are many caveats, not the least of which is the problem of how to evaluate fibers that cross. Other problems include partial volume effects, signal to noise ratio, and validation of fiber tracking. If we can strive to achieve reliable tractography, this would be an important step toward evaluating the

asymmetry of fibers, which would lead to a further understanding of "neural connectivity."

Conclusion

In this study, we proposed a novel method for exploring voxel-based white matter asymmetry. Findings demonstrate anatomical asymmetry of white matter anisotropy in healthy subjects in cingulum bundles, uncinate fasciculus, anterior portion of corpus callosum, the internal capsule, and optic radiation, with similar, albeit more attenuated, findings in schizophrenia.

Acknowledgments

Information on grants. We gratefully acknowledge the support of the Post-doctoral Fellowship Program of Korea Science and Engineering Foundation (KOSEF) (HJP), National Alliance for Research on Schizophrenia and Depression (MK), the National Institutes of Health (K02 MH 01110 and R01 MH 50747 to MES, R01 MH 40799 to RWM, R01 NS 39335 to SEM, and RO3 MH068464-01 to MK), the Department of Veterans Affairs Merit Awards (MES, RWM), and the National Center for Research Resources (11747 to RK and P41-RR13218 to FAJ and CFW).

References

Aboitiz, F., Scheibel, A.B., Fisher, R.S., Zaidel, E., 1992. Fiber composition of the human corpus callosum. Brain Res. 598 (1–2), 143–153.

Akbarian, S., Kim, J.J., Potkin, S.G., Hetrick, W.P. , Bunney Jr., W.E., Jones, E.G. 1996. Maldistribution of interstitial neurons in prefrontal white matter of the brains of schizophrenic patients. Arch. Gen. Psychiatry 53 (5), 425–436.

Alexander, D.C., Pierpaoli, C., Basser, P.J., Gee, J.C., 2001. Spatial transformations of diffusion tensor magnetic resonance images. IEEE Trans. Med. Imag. 20 (11), 1131–1139.

Amunts, K., Jancke, L., Mohlberg, H., Steinmetz, H., Zilles, K., 2000. Interhemispheric asymmetry of the human motor cortex related to handedness and gender. Neuropsychologia 38 (3), 304–312.

Anderson, B., Southern, B.D., Powers, R.E., 1999. Anatomic asymmetries of the posterior superior temporal lobes: a postmortem study. Neuropsychiatry Neuropsychol. Behav. Neurol. 12 (4), 247–254.

Barnea-Goraly, N., Eliez, S., Hedeus, M., Menon, V., White, C.D., Moseley, M., Reiss, A.L., 2003. White matter tract alterations in fragile X syndrome: preliminary evidence from diffusion tensor imaging. Am. J. Med. Genet. 118B (1), 81–88.

Basser, P.J., 1995. Inferring microstructural features and the physiological state of tissues from diffusion-weighted images. NMR Biomed. 8 (7–8), 333–344.

Basser, P.J., Mattiello, J., LeBihan, D., 1994. MR diffusion tensor spectroscopy and imaging. Biophys. J. 66 (1), 259–267.

Beaton, A.A., 1997. The relation of planum temporale asymmetry and morphology of the corpus callosum to handedness, gender, and dyslexia: a review of the evidence. Brain Lang. 60 (2), 255–322.

Buchsbaum, M.S., Tang, C.Y., Peled, S., Gudbjartsson, H., Lu, D., Hazlett, E.A., Downhill, J., Haznedar, M., Fallon, J.H., Atlas, S.W., 1998. MRI white matter diffusion anisotropy and PET metabolic rate in schizophrenia. NeuroReport 9 (3), 425–430.

Burns, J., Job, D., Bastin, M.E., Whalley, H., Macgillivray, T., Johnstone, E.C., Lawrie, S.M., 2003. Structural disconnectivity in schizophrenia: a diffusion tensor magnetic resonance imaging study. Br. J. Psychiatry 182, 439–443.

Cao, Y., Whalen, S., Huang, J., Berger, K.L., DeLano, M.C., 2003. Asymmetry of subinsular anisotropy by in vivo diffusion tensor imaging. Hum. Brain Mapp. 20, 82–90.

Deakin, J.F., Simpson, M.D., 1997. A two-process theory of schizophrenia: evidence from studies in post-mortem brain. J. Psychiatr. Res. 31 (2), 277–295.

Di Virgilio, G., Clarke, S., 1997. Direct interhemispheric visual input to human speech areas. Hum. Brain Mapp. 5 (5), 347–354.

Ebeling, U., von Cramon, D., 1992. Topography of the uncinate fascicle and adjacent temporal fiber tracts. Acta Neurochir. (Wien.) 115 (3–4), 143–148.

Eriksson, S.H., Rugg-Gunn, F.J., Symms, M.R., Barker, G.J., Duncan, J.S., 2001. Diffusion tensor imaging in patients with epilepsy and malformations of cortical development. Brain 124 (Pt. 3), 617–626.

Foong, J., Symms, M.R., Barker, G.J., Maier, M., Miller, D.H., Ron, M.A., 2002. Investigating regional white matter in schizophrenia using diffusion tensor imaging. NeuroReport 13 (3), 333–336.

Galaburda, A.M., LeMay, M., Kemper, T.L., Geschwind, N., 1978a. Right–left asymmetrics in the brain. Science 199 (4331), 852–856.

Galaburda, A.M., Sanides, F., Geschwind, N., 1978b. Human brain. Cytoarchitectonic left-right asymmetries in the temporal speech region. Arch. Neurol. 35 (12), 812–817.

Gazzaniga, M.S., 2000. Cerebral specialization and interhemispheric communication: does the corpus callosum enable the human condition? Brain 123 (Pt. 7), 1293–1326.

Geschwind, N., 1972. Cerebral dominance and anatomic asymmetry. N. Engl. J. Med. 287 (4), 194–195.

Geschwind, N., Galaburda, A.M., 1985a. Cerebral lateralization. Biological mechanisms, associations, and pathology: I. A hypothesis and a program for research. Arch. Neurol. 42 (5), 428–459.

Geschwind, N., Galaburda, A.M., 1985b. Cerebral lateralization. Biological mechanisms, associations, and pathology: II. A hypothesis and a program for research. Arch. Neurol. 42 (6), 521–552.

Geschwind, N., Galaburda, A.M., 1985c. Cerebral lateralization. Biological mechanisms, associations, and pathology: III. A hypothesis and a program for research. Arch. Neurol. 42 (7), 634–654.

Good, C.D., Johnsrude, I., Ashburner, J., Henson, R.N., Friston, K.J., Frackowiak, R.S., 2001. Cerebral asymmetry and the effects of sex and handedness on brain structure: a voxel-based morphometric analysis of 465 normal adult human brains. NeuroImage 14 (3), 685–700.

Gudbjartsson, H., Maier, S.E., Mulkern, R.V., Morocz, I.A., Patz, S., Jolesz, F.A., 1996. Line scan diffusion imaging. Magn. Reson. Med. 36 (4), 509–519.

Guimond, A., Meunier, J., Thirion, J.-P., 2000. Average brain models: a convergence study. Comput. Vis. Image Underst. 77, 192–210.

Guimond, A., Roche, A., Ayache, N., Meunier, J., 2001. Three-dimensional multimodal brain warping using the demons algorithm and adaptive intensity corrections. IEEE Trans. Med. Imag. 20 (1), 58–69.

Guimond, A., Guttmann, C.R.G., Warfield, S.K., Westin, C.-F., 2002. Deformable registration of DT-MRI data based on transformation invariant tensor characteristics. Proceedings of the IEEE International Symposium on Biomedical Imaging (ISBI'02), Washington (DC), USA.

Highley, J.R., Esiri, M.M., McDonald, B., Cooper, S.J., Crow, T.J., 1998a. Temporal-lobe length is reduced, and gyral folding is increased in schizophrenia: a post-mortem study. Schizophr. Res. 34 (1–2), 1–12.

Highley, J.R., Esiri, M.M., McDonald, B., Cortina-Borja, M., Cooper, S.J., Herron, B.M., Crow, T.J., 1998b. Anomalies of cerebral asymmetry in schizophrenia interact with gender and age of onset: a post-mortem study. Schizophr. Res. 34 (1–2), 13–25.

Highley, J.R., McDonald, B., Walker, M.A., Esiri, M.M., Crow, T.J., 1999. Schizophrenia and temporal lobe asymmetry. A post-mortem stereological study of tissue volume. Br. J. Psychiatry 175, 127–134.

Highley, J.R., Walker, M.A., Esiri, M.M., Crow, T.J., Harrison, P.J., 2002. Asymmetry of the uncinate fasciculus: a post-mortem study of normal subjects and patients with schizophrenia. Cereb. Cortex 12 (11), 1218–1224.

Holinger, D.P., Galaburda, A.M., Harrison, P.J., 2000. Cerebral asymmetry. In: Harrison, P.J., Roberts, G.W. (Eds.), The Neuropathology of Schizophrenia. Progress and Interpretation. Oxford Univ. Press, Oxford, pp. 151–172.

Kennedy, D.N., O'Craven, K.M., Ticho, B.S., Goldstein, A.M., Makris, N., Henson, J.W., 1999. Structural and functional brain asymmetries in human situs inversus totalis. Neurology 53 (6), 1260–1265.

Kimura, D., 1973. The asymmetry of the human brain. Sci. Am. 228 (3), 70–78.

Kubicki, M., Westin, C.F., Maier, S.E., Frumin, M., Nestor, P.G., Salisbury, D.F., Kikinis, R., Jolesz, F.A., McCarley, R.W., Shenton, M.E., 2002. Uncinate fasciculus findings in schizophrenia: a magnetic resonance diffusion tensor imaging study. Am. J. Psychiatry 159 (5), 813–820.

Kubicki, M., Westin, C.F., Nestor, P.G., Wible, C.G., Frumin, M., Maier, S.E., Kikinis, R., Jolesz, F.A., McCarley, R.W., Shenton, M.E., 2003. Cingulate fasciculus integrity disruption in schizophrenia: a magnetic resonance diffusion tensor imaging study. Biol. Psychiatry 54 (11), 1171–1180.

Lancaster, J.L., Kochunov, P.V., Thompson, P.M., Toga, A.W., Fox, P.T., 2003. Asymmetry of the brain surface from deformation field analysis. Hum. Brain Mapp. 19 (2), 79–89.

Lim, K.O., Hedehus, M., Moseley, M., de Crespigny, A., Sullivan, E.V., Pfefferbaum, A., 1999. Compromised white matter tract integrity in schizophrenia inferred from diffusion tensor imaging. Arch. Gen. Psychiatry 56 (4), 367–374.

Lin, C.C., Mudholkar, G.S., 1980. A simple test for normality against asymmetric alternatives. Biometrika 67, 455–461.

Maier, S.E., Gudbjartsson, H., Patz, S., Hsu, L., Lovblad, K.O., Edelman, R.R., Warach, S., Jolesz, F.A., 1998. Line scan diffusion imaging: characterization in healthy subjects and stroke patients. AJR Am. J. Roentgenol. 171 (1), 85–93.

Makris, N., Meyer, J.W., Bates, J.F., Yeterian, E.H., Kennedy, D.N., Caviness, V.S., 1999. MRI-Based topographic parcellation of human cerebral white matter and nuclei II. Rationale and applications with systematics of cerebral connectivity. NeuroImage 9 (1), 18–45.

Mamata, H., Mamata, Y., Westin, C.F., Shenton, M.E., Kikinis, R., Jolesz, F.A., Maier, S.E., 2002. High-resolution line scan diffusion tensor MR imaging of white matter fiber tract anatomy. AJNR Am. J. Neuroradiol. 23 (1), 67–75.

McDonald, B., Highley, J.R., Walker, M.A., Herron, B.M., Cooper, S.J., Esiri, M.M., Crow, T.J., 2000. Anomalous asymmetry of fusiform and parahippocampal gyrus gray matter in schizophrenia: a postmortem study. Am. J. Psychiatry 157 (1), 40–47.

Moffat, S.D., Hampson, E., Lee, D.H., 1998. Morphology of the planum temporale and corpus callosum in left handers with evidence of left and right hemisphere speech representation. Brain 121 (Pt. 12), 2369–2379.

Mohr, B., Heim, S., Pulvermuller, F., Rockstroh, B., 2001. Functional asymmetry in schizophrenic patients during auditory speech processing. Schizophr. Res. 52 (1–2), 69–78.

Nestor, P.G., Shenton, M.E., Wible, C., Hokama, H., O'Donnell, B.F., Law, S., McCarley, R.W., 1998. A neuropsychological analysis of schizophrenic thought disorder. Schizophr. Res. 29 (3), 217–225.

Park, H.J., Kubicki, M., Shenton, M.E., Guimond, A., McCarley, R.W., Maier, M., Kikinis, R., Jolesz, F.A., Westin, C.-F., 2003a. Spatial normalization of diffusion tensor MRI using multiple channels. NeuroImage 20 (4), 1995–2009.

Park, H.J., Westin, C.-F., Brun, A., Kubicki, M., McCarley, R.W., Shenton, M.E., 2003b. A method for hemispheric asymmetry of white matters using diffusion tensor MRI. Proceedings of Human Brain Mapping 2003, New York, USA, Neuroimage S(918).

Peled, S., Gudbjartsson, H., Westin, C.F., Kikinis, R., Jolesz, F.A., 1998. Magnetic resonance imaging shows orientation and asymmetry of white matter fiber tracts. Brain Res. 780 (1), 27–33.

Pujol, J., Lopez-Sala, A., Deus, J., Cardoner, N., Sebastian-Galles, N., Conesa, G., Capdevila, A., 2002. The lateral asymmetry of the human brain studied by volumetric magnetic resonance imaging. NeuroImage 17 (2), 670–679.

Rockstroh, B., Kissler, J., Mohr, B., Eulitz, C., Lommen, U., Wienbruch, C., Cohen, R., Elbert, T., 2001. Altered hemispheric asymmetry of auditory magnetic fields to tones and syllables in schizophrenia. Biol. Psychiatry 49 (8), 694–703.

Rosen, G.D., Sherman, G.F., Galaburda, A.M., 1993. Neuronal subtypes and anatomic asymmetry: changes in neuronal number and cell-packing density. Neuroscience 56 (4), 833–839.

Rugg-Gunn, F.J., Eriksson, S.H., Symms, M.R., Barker, G.J., Duncan, J.S., 2001. Diffusion tensor imaging of cryptogenic and acquired partial epilepsies. Brain 124 (Pt. 3), 627–636.

Sommer, I.E., Ramsey, N.F., Kahn, R.S., 2001. Language lateralization in schizophrenia, an fMRI study. Schizophr. Res. 52 (1–2), 57–67.

Sowell, E.R., Thompson, P.M., Rex, D., Kornsand, D., Tessner, K.D., Jernigan, T.L., Toga, A.W., 2002. Mapping sulcal pattern asymmetry and local cortical surface gray matter distribution in vivo: maturation in perisylvian cortices. Cereb. Cortex 12 (1), 17–26.

Springer, S.P., Deutsch, G., 1998. Left Brain, Right Brain: Perspectives From Cognitive Neuroscience Freeman and Co. Worth Publishers, USA.

Takahashi, T., Kawasaki, Y., Kurokawa, K., Hagino, H., Nohara, S., Yamashita, I., Nakamura, K., Murata, M., Matsui, M., Suzuki, M., Seto, H., Kurachi, M., 2002. Lack of normal structural asymmetry of the anterior cingulate gyrus in female patients with schizophrenia: a volumetric magnetic resonance imaging study. Schizophr. Res. 55 (1–2), 69–81.

Toga, A.W., Thompson, P.M., 2001. Maps of the brain. Anat. Rec. 265 (2), 37–53.

Toga, A.W., Thompson, P.M., 2003. Mapping brain asymmetry. Nat. Rev. Neurosci. 4 (1), 37–48.

Turetsky, B., Cowell, P.E., Gur, R.C., Grossman, R.I., Shtasel, D.L., Gur, R.E., 1995. Frontal and temporal lobe brain volumes in schizophrenia. Relationship to symptoms and clinical subtype. Arch. Gen. Psychiatry 52 (12), 1061–1070.

Watkins, K.E., Paus, T., Lerch, J.P., Zijdenbos, A., Collins, D.L., Neelin, P., Taylor, J., Worsley, K.J., Evans, A.C., 2001. Structural asymmetries in the human brain: a voxel-based statistical analysis of 142 MRI scans. Cereb. Cortex 11 (9), 868–877.

Wechsler, D., 1997a. Wechsler Adult Intelligence Scale Psychological Corp., San Antonio, TX (Harcourt).

Wechsler, D., 1997b. The Wechsler Memory Scale Psychological Corp., San Antonio, TX (Harcourt).

Westbury, C.F., Zatorre, R.J., Evans, A.C., 1999. Quantifying variability in the planum temporale: a probability map. Cereb. Cortex 9 (4), 392–405.

Westin, C.F., Maier, S.E., Mamata, H., Nabavi, A., Jolesz, F.A., Kikinis, R., 2002. Processing and visualization for diffusion tensor MRI. Med. Image Anal. 6 (2), 93–108.

Youn, T., Park, H.J., Kim, J.J., Kim, M.S., Kwon, J.S., 2003. Altered hemispheric asymmetry and positive symptoms in schizophrenia: equivalent current dipole of auditory mismatch negativity. Schizophr. Res. 59 (2–3), 253–260.

Zhou, S.Y., Suzuki, M., Hagino, H., Takahashi, T., Kawasaki, Y., Nohara, I., Yamashita, I., Seto, H., Kurachi, M., 2003. Decreased volume and increased asymmetry of the anterior limb of the internal capsule in patients with schizophrenia. Biol. Psychiatry 54 (4), 427–436.